Spectrochimica Acta, Vol. 30A, pp. 1771 to 1786. Pergamon Press 1974. Printed in Northern Ireland

Vibrational studies of molybdates, tungstates and related compounds—III. Ordered cubic perovskites $A_2B^{II}B^{VI}O_6$

M. Liegeois-Duyckaerts and P. Tarte
University of Liège, Institute of Chemistry, 4000–Sart Tilman par Liège 1, Belgium

(*Received* 25 *November* 1973)

Abstract—Most of the bands predicted by a group theoretical analysis have been observed in the i.r. and Raman spectra of a number of ordered, cubic perovskites $A_2B^{II}B^{VI}O_6$. With the help of cartesian symmetry coordinates, and from the wealth of experimental data including ^{24}Mg—^{26}Mg, ^{40}Ca—^{44}Ca and ^{122}Te—^{130}Te isotopic frequencies, it appears that the separation of the observed vibrations in internal and external modes is a good approximation for the high-frequency bands, which are assigned to the stretching vibrations of the $B^{VI}O_6$ octahedron. This approximation is not so satisfactory for the corresponding bending vibrations, since these vibrations may be more or less mixed up with translational, external modes which belong to the same symmetry species (T_{1u} in i.r.; T_{2g} in Raman). The behaviour of the totally symmetric A_{1g} mode has been investigated in some detail: its frequency is predominantly determined by the nature of the hexavalent B^{VI} cation; but it is also influenced by the nature of the bivalent B^{II} octahedral cation, acting through its bonding force and ionic radius, and by the size of the large A cation, because of its influence on the B^{II}—O distance. Abnormal values of the A_{1g} frequency are observed when the B^{II} cation is rather large: this is qualitatively explained by a displacement of the oxygen towards the B^{VI} cation, with or without distortion of the structure.

Introduction

The structure of the ideal, most simple perovskites ABX_3 (X = O or F), may be described as a close cubic packing of AX_3 sheets, the octahedral interstices of which are occupied by the small B cations. The introduction, in the structure, of 2 cations B and B′ differing by their chemical nature and their electrostatic charge, leads to various derived structures, depending on (1) the number and distribution of the B and B′ cations, and (2) the packing type of the AX_3 sheets. The type of packing determines the linking mode of the BO_6 and $B'O_6$ octahedra in the cubic close packing, the octahedra are linked by their apexes, whereas they are sharing faces in the hexagonal close packing [1]. We shall consider here the compounds corresponding to the cubic close packing. The so-called "hexagonal perovskites", with a mixed cubic-hexagonal close packing, will be discussed in a next paper.

A further discrimination must be introduced within the group of the ordered perovskites $A_2BB'O_6$ characterized by a cubic close packing. The compounds with the highest crystal symmetry are cubic, space group $Fm3m$. But the introduction, in the crystal lattice, of, either A cations smaller than oxygen (such as Sr or Ca), or B cations too large for the space available in the octahedral holes, leads to a distortion of the lattice and a lowering of the symmetry, which may be

[1] L. Katz, R. Ward, *Inorg. Chem.* **3**, 205 (1964).

rhombohedral, tetragonal, orthorhombic or even monoclinic. Most of these distorted phases have been investigated by X-ray powder diffractometry; as a consequence, the oxygen positions are not determined with sufficient accuracy, and the space groups of these phases are generally unknown.

EXPERIMENTAL

Synthesis of the compounds

All the compounds have been synthesized by solid state reaction. The stoichiometric mixture of the necessary oxides and carbonates is heated up to a convenient temperature (Table 1), either in air, or in oxygen. For most of the tungstates and

Table 1. Synthesis of the compounds

Compounds	Initial mixture: A = Sr, Ba, Pb; B = Mg, Ni, Co, Cu, Zn, Cd, Ca, Sr, Ba.	Temperature	Remarks
$A_2B^{II}U^{VI}O_6$	$2ACO_3 + BCO_3$(or BO) + $UO_2(C_2H_3O_2)_2 \cdot 2H_2O$	1100°C	Hydrolysis $\rightarrow AUO_4$
$A_2B^{II}W^{VI}O_6$	$2ACO_3 + BCO_3(BO) + WO_3$	1200–1400°C	Metastable $\rightarrow AWO_4$
$A_2B^{II}Mo^{VI}O_6$	$2ACO_3 + BCO_3(BO) + MoO_3$	$\rightarrow$500°C $\rightarrow$ 1000–1300°C	Metastable $\rightarrow AMoO_4$
$A_2B^{II}Te^{VI}O_6$	$2ACO_3 + BCO_3(BO) + TeO_2$ 2PbO	$\rightarrow$600°C $\rightarrow$ 1100°C	

molybdates, a scheelite phase (such as $BaWO_4$) is first formed, and several grinding and heating cycles are necessary before a single, homogeneous perovskite phase is obtained.

On the other hand, some compounds are sensitive to water vapour, the hydrolysis process being the most easy with the uranates. The purity of the compounds has been checked by the combined use of X-ray diffractometry, and vibrational spectroscopy (i.r. and Raman). Both i.r. and Raman spectra are rather sensitive to the presence of impurities resulting from either some hydrolysis, or incomplete reaction. The impurities (e.g. a scheelite phase such as $BaWO_4$) have strong absorption or diffusion peaks in a fairly high frequency region (950–900 cm^{-1} for the scheelite phases) where they are not obscured by the vibrational spectrum of the perovskite phase.

Spectra

The i.r. spectra have been investigated with a Beckman i.r. 12 (down to 200 cm^{-1}) and a CAMECA SI 36 (200–50 cm^{1}) spectrometers. The pressed disc technique (KI or polythene discs, depending on the spectral region) has been used throughout. The Raman spectra were obtained with a Coderg PHO double monochromator equipped with a 50 mW He–Ne laser (Spectra-Physics).

VIBRATIONAL THEORY FOR THE ORDERED, CUBIC $A_2BB'O_6$ PEROVSKITES

The ordered $A_2BB'O_6$ perovskites with the highest symmetry are cubic, space group Fm3m, with 4 formula units in the non-primitive crystal cell. The atomic

positions in this crystal cell are given in Table 2 and Fig. 1. The primitive Bravais cell is obtained by a basic translation from the apex to the centre of the faces of the cube, and conversely: it is rhombohedral with 1 formula unit in the primitive

Table 2. Atomic positions in the cubic crystal cell Fm3m

Atom	Wyckoff sites	Site symmetry	Coordinates of equivalent positions
A	8c	T_d	$\frac{1}{4}, \frac{1}{4}, \frac{1}{4}$; $\frac{3}{4}, \frac{3}{4}, \frac{3}{4}$
B	4b	O_h	$\frac{1}{2}, \frac{1}{2}, \frac{1}{2}$
B′	4a	O_h	0, 0, 0
O	24e	C_{4v}	$x, 0, 0$; $0, x, 0$; $0, 0, x$; $\bar{x}, 0, 0$; $0, \bar{x}, 0$; $0, 0, \bar{x}$. †Translations: $0, \frac{1}{2}, \frac{1}{2}$; $\frac{1}{2}, 0, \frac{1}{2}$; $\frac{1}{2}, \frac{1}{2}, 0$

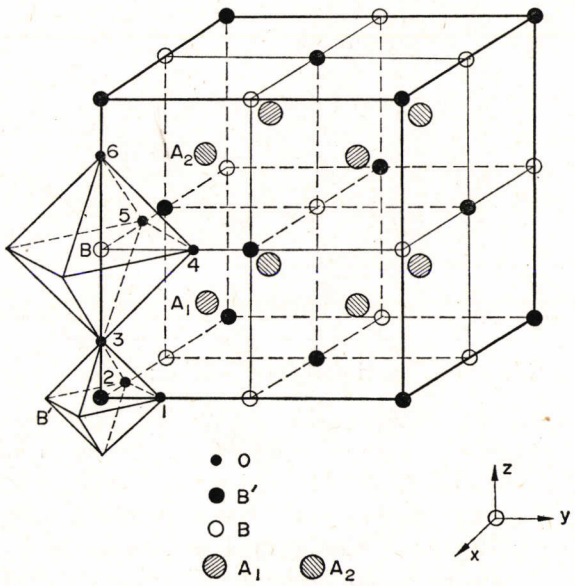

Fig. 1. Cubic crystal cell of the ordered $A_2BB'O_6$ perovskites (B = bivalent; B′ = hexavalent cation). Numbering of ten non equivalent atoms: A_1, A_2, B, B′ atoms and six oxygen atoms with subscripts 1–6. The cartesian coordinates system is chosen so that the x, y, z axis are along the fourfold crystal cell axis.

cell. On the basis of this Bravais cell, the vibrational modes of the crystal have been investigated by factor group analysis. This leads, for $k = 0$, to the irreducible representation:

$$\Gamma_i = A_{1g} + E_g + T_{1g} + 2T_{2g} + 5T_{1u} + T_{2u}$$

from which $1T_{1u}$ (acoustic), the T_{1g} and T_{2u} (both inactive) modes should be subtracted. Finally, 4 Raman active ($1A_{1g} + 1E_g + 2T_{2g}$) and 4 i.r. active ($4T_{1u}$) modes are expected.

The displacements of the atoms have been evaluated on the basis of cartesian symmetry coordinates (Table 3). These relations give useful information about the

Table 3. Cartesian symmetry coordinates

$$S^{A_{1g}} = \frac{1}{\sqrt{6}}(x_2 - x_5 + y_4 - y_1 + z_6 - z_3)$$

$$S^{E_g} = \frac{1}{2\sqrt{3}}(2x_2 - 2x_5 + y_1 - y_4 + z_3 - z_6)$$

$$= \tfrac{1}{2}(y_1 - y_4 + z_6 - z_3)$$

$$S_a^{T_{2g}} = \tfrac{1}{2}(x_1 - x_4 + y_5 - y_2)$$

$$= \tfrac{1}{2}(z_1 - z_4 + y_3 - y_6)$$

$$= \tfrac{1}{2}(z_2 - z_5 + x_6 - x_3)$$

$$S_b^{T_{2g}} = \frac{1}{\sqrt{2}}(x_{A_1} - x_{A_2})$$

$$= \frac{1}{\sqrt{2}}(y_{A_1} - y_{A_2})$$

$$= \frac{1}{\sqrt{2}}(z_{A_1} - z_{A_2})$$

$$S_1^{T_{1u}} = \frac{1}{\sqrt{2}}(x_{A_1} + x_{A_2})$$

$$S_2^{T_{1u}} = x_B$$

$$S_3^{T_{1u}} = x_{B'}$$

$$S_4^{T_{1u}} = \tfrac{1}{2}(x_1 + x_3 + x_4 + x_6)$$

$$S_5^{T_{1u}} = \frac{1}{\sqrt{2}}(x_2 + x_5)$$

The same relations give the coordinates along the y and the z axes respectively.

factors which determine the vibrational frequencies:

(1) During the vibrations of A_{1g} and E_g symmetry, all the cations are necessarily at rest, and there will be no cationic mass effect. Since, in addition, the oxygen atoms are moving along the B—O—B′ axis, the corresponding frequencies will be primarily determined by the B—O and B′—O bonding forces.

(2) Besides the oxygen atoms, the large A cations are allowed to move during the T_{2g} vibrations. The corresponding frequencies may be more or less influenced by the mass of A, and by the A—O binding energy.

(3) The situation is more complex for the i.r. active vibrations, since all these vibrations belong to the same representation T_{1u}, and all atoms are allowed to move.

The problem may be more or less simplified by considering the existence of internal vibrations of the octahedral $B'O_6$ group, where B′ is the cation with the highest valency (6 + in most of the compounds reported in this paper).

INFRARED SPECTRA AND ASSIGNMENTS.

The i.r. spectra exhibit the 4 bands predicted by the factor group analysis. The 2 "high-frequency" bands (700–350 cm^{-1}) are generally broad and asymmetric (except for tellurates) whereas the 2 low-frequency bands are weaker and sharper. Since these 4 modes belong to the same representation T_{1u} and since all atoms are allowed to move during these vibrations, the investigation of isotopic species is probably the most reliable method to find out the atoms which are *predominantly*

participating to a vibration of given frequency. The results given by the investigation of isotopic species with ^{122}Te–^{130}Te, ^{24}Mg–^{26}Mg and ^{40}Ca–^{44}Ca are collected in Table 4.

Table 4. Isotopic shifts and infrared bands assignments

Compound		Internal $\nu_3(B^{VI}O_6)$	Internal $\nu_4(B^{VI}O_6)$	External $T(B^{II})$	External T
Ba_2MgTeO_6	^{24}Mg	650	410	313	166
				8	(−2)
	^{26}Mg	650	410	305	168
	^{122}Te	650	410	312	167
		0	0		
	^{130}Te	650	410	312	167
Ba_2CaTeO_6	^{40}Ca	680	402	291	~140
				8	(5)
	^{44}Ca	680	402	283	~135
	^{122}Te	680	404	292	142
		2	3		(3)
	^{130}Te	678	401	292	139
Ba_2CdTeO_6	^{122}Te	664	389	202	128[5]
		2	4		
	^{130}Te	662	385	202	129[5]
Sr_2MgTeO_6	^{24}Mg	715	413	351	~168
				11	(−2)
	^{26}Mg	715	413	340	~170
Ba_2MgWO_6	^{24}Mg	618	381	321	149
				7	(−3)
	^{26}Mg	618	381	314	152
Ba_2MgUO_6	^{24}Mg	604	341	283	129
			11	3	
	^{26}Mg	604	330	280	129
Ba_2CaWO_6	^{40}Ca	620	338	291	127
				9	
	^{44}Ca	620	338	282	127

Assignment of the 2 "high-frequency" bands

The highest-frequency band (700–600 cm^{-1}) is not sensitive to the mass of the small bivalent cation (Mg or Ca); on the other hand, the mass effect of tellurium on this frequency is not clear-cut, since the ^{122}Te–^{130}Te isotopic shifts are small or very small (0–4 cm^{-1}), and some of them are nearly within the limits of experimental error. It is also well known that the absorption bands related to translations of the heavy divalent cation (Ba or Sr) are located in the low-frequency region, near or below 200 cm^{-1}. It may be concluded that the highest frequency band is essentially related to a motion of the oxygen anions, with a small contribution of the hexavalent, octahedral cation. Indeed, the frequency values quoted in Table 4 are in good agreement with the antisymmetric stretching frequencies of TeO_6, WO_6 . . . "isolated" octahedra, and this high-frequency band may be assigned to an internal mode, namely the antisymmetric stretch, of the TeO_6, WO_6 . . . octahedral group.

The same considerations hold for the second band, in the 400–340 cm^{-1} region, which is thus assigned to the internal, antisymmetric bending mode of the same octahedral group. There is, however, a very noticeable exception, namely Ba_2MgUO_6, for which this second band is strongly shifted by the ^{24}Mg–^{26}Mg isotopic replacement.

This may be simply explained by the fact that the rather low frequency of the UO_6 bending mode (340–300 cm^{-1} in the other uranates) is of the same order of magnitude that the frequency corresponding to the translational motion of the light Mg cation. Since both modes belong to the same representation T_{1u}, there is a strong mixing between them. This "mixing" simply implies that the real normal modes are described by a more complex linear combination of the symmetry coordinates. Thus, it appears that the separation of the vibrational modes into internal and external ones is a satisfactory approximation for the highest frequency corresponding to the stretching motion of the $B'O_6$ octahedron, but is not necessarily valid for the corresponding bending mode, since this bending mode is more liable to mix up with external, translational modes. A similar situation has been observed for the molybdates and germanates spinels, where the mixing of the GeO_4 bending mode with a cation translation has also been evidenced with the help of isotopic shifts [2].

The diffuse and asymmetric shape of these bands has already been mentioned. This behaviour may tentatively be explained, either by a splitting related to some deformation of the crystal lattice with respect to the ideal cubic symmetry [3], or by surface effects.

We do not believe that the observed broadening of the high-frequency bands is related to a deformation of the crystal lattice, first because there is good combined evidence from X-ray diffractometry, Raman and i.r. spectroscopy that all compounds reported in Table 5 really belong to the cubic space group Fm3m; and second, because the investigation of compounds of lower symmetry shows that the high-frequency i.r. bands are not very sensitive to the deformation; instead, any lowering of the site symmetry has a marked influence on the Raman active, T_{2g}, bending mode. Thus, in the vibrational spectrum, any significant departure from the ideal cubic symmetry would appear *first* in the Raman active T_{2g} bending mode, which is not the case for the compounds discussed in this paper.

Thus, there remains the explanation based on surface effects. This problem has been carefully investigated in some simple perovskites such as $KNiF_3$, $KMgF_3$ and $SrTiO_3$ [4]. For these compounds, there is a large frequency difference between the corresponding longitudinal optic and transversal optic modes, and thus, in a powder spectrum, the shape and the position of the "absorption" bands strongly depend on the size and shape of the particles, and on the refractive index of the dispersive medium. In conclusion, there is no need to consider any deformation of the crystal lattice for the compounds under discussion.

Origin of the low frequency bands

Out of the 2 low frequency bands, one (in the 350–200 cm^{-1} region) is very sensitive to the mass of the B^{II}, bivalent octahedral cation (Mg, Ca . . .): this appears clearly from the isotopic data quoted in Table 4 (the only exception being Ba_2MgUO_6; this case has already been discussed). The mass influence of the other cations is small or negligible. This is shown, for the large A^{II} cation, by the nearly identical

[2] P. TARTE, J. PREUDHOMME, *Spectrochim. Acta* **28A,** 69 (1972).
[3] A. F. CORSMIT, H. E. HOEFDRAAD and G. BLASSE, *J. Inorg. Nucl. Chem.* **34,** 3401 (1972).
[4] R. RUPPIN and R. ENGELMAN, *Rep. Prog. Phys.* **33,** 149 (1970).

Table 5. Raman and infrared frequencies and general assignments

		Internal modes					External modes		
	a_0(Å)	$A_{1g}(\nu_1)$	$E_g(\nu_2)$	$T_{1u}(\nu_3)$	$T_{1u}(\nu_4)$	$T_{2g}(\nu_5)$	T_{1u}	T_{1u}	T_{2g}
$(BaSr)MgWO_6$	$8{\cdot}00_0$	847		656	380	446	~350	150	128
Ba_2NiWO_6	$8{\cdot}06_6$[5]	816		610	382	434	234	148	128
Ba_2CoWO_6	$8{\cdot}09_8$[5]	800		609	367	c	227	144	c
Ba_2MgWO_6	$8{\cdot}09_9$	813		618	381	441	321	149	126
Ba_2ZnWO_6	$8{\cdot}11_6$[5]	822		605	357	431	208	137	124
Ba_2CdWO_6	$8{\cdot}34_0$	845		620	340	405	186	120	106
Ba_2CaWO_6	$8{\cdot}40_0$	838		620	338	413	291	127	105
$(BaSr)CaWO_6$	$8{\cdot}29_5$	828		614	343	423	291	137	106/~100
Ba_2NiMoO_6	$8{\cdot}04_3$[6]	c		590	395	c	250	158	c
Ba_2CoMoO_6	$8{\cdot}08_6$[6]	c		590	375	c	240	152	c
Ba_2MgMoO_6	$8{\cdot}08_0$	779		605	387	438	330	164	127
Ba_2ZnMoO_6	$8{\cdot}09_5$	785		594	385	428	226	sh	124
Ba_2CdMoO_6	$8{\cdot}33_0$	808	~514	615	350	401	208	120	106
Ba_2CaMoO_6	$8{\cdot}37_5$	802		603	360	407	302	134	104
Sr_2MgTeO_6	$7{\cdot}90_5$	782		715	413	431	351	~168	140
$(PbSr)MgTeO_6$	$7{\cdot}95_5$	775	~477	700	402	366/419	337	160/~125	51/131
$(Pb_{1.5}Sr_{0.5})MgTeO_6$	$7{\cdot}98_5$	766	~580/~473	693	395	362/~391	335	148	54/sh
Pb_2MgTeO_6	$7{\cdot}99_5$	761	570	685	373	359	315	127	60
$(BaSr)MgTeO_6$	$7{\cdot}99_5$	758		695	410	420	338	170	104/131
$(Pb_{1.5}Ba_{0.5})MgTeO_6$	$8{\cdot}03_4$	753	565/~470	675	395	364/~396	320	150	52
$(PbBa)MgTeO_6$	$8{\cdot}07_5$	742	~470	666	409	364/407	320	163/~145	45/126
$(BaLa)LiTeO_6$	8.04_4	716		675	417	428	350	171	123
Ba_2MgTeO_6	$8{\cdot}11_0$	724		650	410	414	313	166	132
Ba_2CdTeO_6	$8{\cdot}33_5$	745	561	667	392	385	204	129	111
$(BaLa)NaTeO_6$	$8{\cdot}27_0$	716		677	410	430	~272	~165	114
Ba_2CaTeO_6 *	$8{\cdot}39_5$	748	608	680	402	402	291	~140	109
Ba_2NiUO_6	$8{\cdot}33_4$[7]	743		595	315	350	222	129	c
Ba_2CoUO_6	$8{\cdot}37_0$[7]	c		580	305	c	220	120	c
Ba_2MgUO_6	$8{\cdot}37_9$[7]	753		604	341	352	283	129	108
Ba_2ZnUO_6	$8{\cdot}39_3$[7]	762		600	310	348	191	124	107

Sh: shoulder
c: colored compounds
*: Ba_2NiTeO_6 as well as the Co, Cu, Zn compounds are hexagonal perovskites.

frequencies of Pb_2MgTeO_6 and Ba_2MgTeO_6 (315 and 313 cm^{-1} respectively). And this is suggested, for the octahedral B^{VI} cation, by the lack of a significant ^{122}Te–^{130}Te isotopic shift, and also by the fact that the frequencies for the corresponding molybdates and tungstates are not very different. It will be noticed, however, that the frequencies of the molybdates are slightly, but systematically higher than those of the corresponding tungstates.

Since the restoring force is generally slightly smaller for Mo—O than for W—O bonds, this effect suggests a small mass influence of the hexavalent cation. It may be concluded that the frequency under discussion is predominantly (but not uniquely) determined by a translation of the bivalent, octahedral B^{II} cation, with of course some compensating motion of the oxygen anions, as represented in Fig. 2.

Finally, the situation is considerably more complicated for the lowest frequency band. No conclusion can be deduced from the isotopic data, since the observed shifts are too small (with respect to the broadness of the bands) to be significant. Furthermore, no general trend may be evidenced from the numerous data quoted in Table 5,

[5] E. J. Fresia, L. Katz, R. Ward, *J. Am. Chem. Soc.* **81,** 4783 (1959).
[6] L. H. Brixner, *J. Phys. Chem.* **64,** 165 (1960).
[7] A. W. Sleight, R. Ward, *Inorg. Chem.* **1,** 790 (1962).

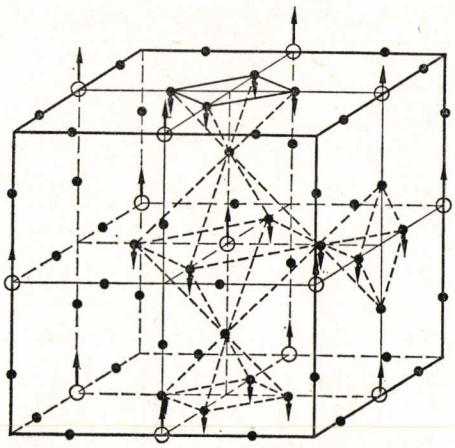

Fig. 2. Normal coordinate $Q_z^{T_{1u}}$ along z axis. $Q^{T_{1u}} = t(z_B) - u(z_1 + z_2 + z_4 + z_5)$.

and tentative interpretations deduced from the consideration of a given pair of compounds may be in contradiction with the behaviour of some other compounds. Without going into much details, we just quote here a few examples of these difficulties:

(1) The observed frequencies are, in most cases at least, slightly but significantly lower for the tungstates than for the corresponding molybdates, and this would suggest at least a small displacement of the hexavalent cation. However, the frequency is the same (120 cm^{-1}) for the cadmium compounds Ba_2CdWO_6 and Ba_2CdMoO_6; and, in addition, the frequencies are slightly higher for the tellurates than for the corresponding molybdates.

(2) A significant displacement of the large A cation is strongly suggested by the frequency values observed for Ba_2MgTeO_6 and Pb_2MgTeO_6 (166 and 127 cm^{-1} respectively), and also by the 2-modes behaviour observed for (Pb, Sr) $MgTeO_6$ and (Pb, Ba) $MgTeO_6$ solid solutions. But here again, this is not supported by the nearly equal frequency values given by Sr_2MgTeO_6 and Ba_2MgTeO_6 (168 and 166 cm^{-1} respectively).

From these apparently contradictory results, it may be tentatively concluded that this lowest-frequency mode is related to some complex translations of the different cations, whose relative amplitudes are different from a compound to another. No experimental information is available about the displacements of the oxygen atoms: this would require the investigation of ^{18}O compounds.

RAMAN DATA AND ASSIGNMENTS

General considerations

Since the 4 Raman active modes are distributed into 3 different symmetry classes, polarization data on monocrystals should give an unequivocal basis for their assignment. Nevertheless, in the actual case of powder data, the consideration

of the cartesian symmetry coordinates (Table 3) and of the relative bonding forces gives useful information about the origin of the bands.

During the A_{1g} vibration, all the cations are at rest, and the oxygen displacements (Table 3) may be represented as in Fig. 3: this is clearly the totally symmetric stretch of the $B^{VI}O_6$ octahedron in the internal modes approximation. This approximation is justified by the i.r. results (see above) and by the fact that the B^{VI}—O bond is by far the strongest bond in the crystal. This type of vibration should give a strong Raman peak at a relatively high frequency: it is thus assigned to the strong peak which appears consistently in all Raman spectra in the 850–700 cm^{-1} region (Table 5). Quite similar considerations may be applied to the E_g mode, which appears as the antisymmetric (with respect to the ternary C_3 axis of the octahedron) stretch of the $B^{VI}O_6$ octahedron.

The situation is more complicated for the 2 T_{2g} modes since, in addition to the oxygen anions, the heavy A cations are also allowed to move. However, it can be expected that the corresponding frequencies should be lower than those related to the A_{1g} and E_g modes.

Behaviour of the A_{1g} *mode*

The A_{1g} mode always appears as a strong peak in the 850–700 cm^{-1} region; it is not sharp, and generally asymmetric. It has already been pointed out that this mode corresponds to a displacement of the oxygen atoms along the B^{II}—O—B^{VI} axis. Thus, its frequency should be primarily determined by the B^{VI}—O and B^{II}—O distances and bonding forces, and thus by the chemical nature of the B^{VI} and B^{II} octahedral cations.

Now, as far as the distances are concerned, 2 points should be kept in mind:

(1) The existing data on the position parameter x of the oxygen are rather scarce, and it is impossible to investigate separately the influence of the B^{VI}—O and B^{II}—O distances on the vibrational frequencies. Instead, we have considered the influence of the cell parameter a_0 as a measure of the total B^{VI}—O—B^{II} distance.

(2) Although the large A cation does not participate by itself to the A_{1g} mode, its influence on the distances cannot be neglected. When the position of the oxygen has been determined with sufficient accuracy, it is found that, besides its influence on the cell parameter a_0, the size of the A cation also have a specific influence on the B^{II}—O distance, but not on the B^{VI}—O distance. This clearly appears in the data quoted for Ba_2NiWO_6 and Sr_2NiWO_6 in Table 6. This is not unexpected, since the oxygen atom is more tightly bonded to the B^{VI} than to the B^{II} cation, and any change in the bond distances is likely to be essentially localized on the weakest bonds. This leads us to consider first the influence of the nature of the A cation on the A_{1g} frequency.

Influence of the nature of the large A *cation*

This influence cannot be investigated with the tungstates, the molybdates and the uranates, since these cubic perovskites are essentially restricted to the Ba compounds; but the tellurates A_2MgTeO_6, where A may be Sr, Pb or Ba, are

Table 6. Data on the positions of the oxygen atoms

Compound	Unit cell parameter a_0 (Å)	Oxygen position x	distance B′–O d_1 (Å)	distance B–O d_2 (Å)	Difference between ionic radii $(B–B')$ [14] Δr (Å)
Ba_2NiWO_6	$8{\cdot}08_6$	0·240 [9]	$1{\cdot}93_5$	2.10	0·10
Sr_2NiWO_6			$1{\cdot}92_5$ [10]	2·02 [10]	0·10
Ba_2CoWO_6	$8{\cdot}09_8$	0·238 [9]	1·93	2·12	0·13
Ba_2BaWO_6	$8{\cdot}63_0$	0·210 [11]	1·81	2·50	0·76
Ba_2BaMoO_6	$8{\cdot}60_0$	0·210 [11]	1·81	2·49	0·76
βSr_2SrMoO_6	$8{\cdot}24_0$	0·220 [11]	1·81	2·31	0·56
Cs_2NaYF_6	$9{\cdot}07_5$	$0{\cdot}25_0$ [12]	2·27	2·17	0·13
Cs_2KYF_6	$9{\cdot}44_5$	$0{\cdot}22_5$ [12]	$2{\cdot}12_5$	2·60	0·49
Cs_2RbYF_6	$9{\cdot}62_5$	$0{\cdot}22_0$ [12]	2·12	$2{\cdot}69_5$	0·60

quite convenient. We can now bring together the following points (Table 5 and Fig. 4):

(1) The relationship between the A_{1g} frequency and the cell parameter a_0 is nearly linear. There is no anomaly related to the presence of the Pb cation (as it is the case in the scheelites [8]) and it may be inferred that there is no specific influence of the chemical nature (in fact, of the electronic structure) of the A cation.

(2) The influence of the A cation may thus be considered as being restricted to an overall effect of interatomic distances and cell parameter a_0.

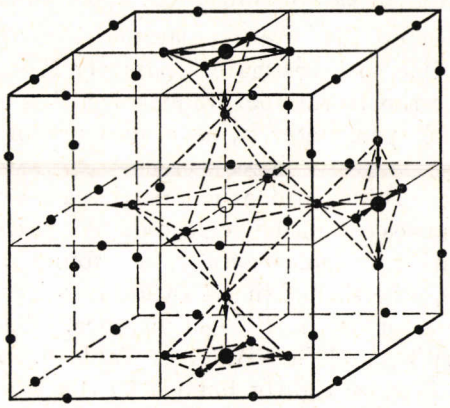

Fig. 3. Symmetry coordinate $S^{A_{1g}} = 1/\sqrt{6}\,(x_2 - x_5 + y_4 - y_1 + z_6 - z_3)$.

[8] M. LIEGEOIS-DUYCKAERTS and P. TARTE, *Spectrochim. Acta* **28A**, 2037 (1972).
[9] D. E. COX, G. SHIRANE and B. C. FRAZER, *J. Appl. Phys.* **38**, 1459 (1967).
[10] P. KÖHL, U. MÜLLER and D. REINEN, *Z. Anorg. Allg. Chem.* **392**, 124 (1972).
[11] R. SABATIER, M. WATHLE, J. P. BESSE and G. BAUD, *C. R. Acad. Sc. Paris* **271**, 368 (1970).
[12] A. VEDRINE, J. P. BESSE, G. BAUD and M. CAPESTAN, *Rev. Chim. Min.* **7**, 593 (1970).
[13] D. REINEN, *Theoret. Chim. Acta* (Berl.) **5**, 312 (1966).
[14] R. D. SHANNON and C. T. PREWITT, *Acta Cryst.* **B25** 925 (1969).

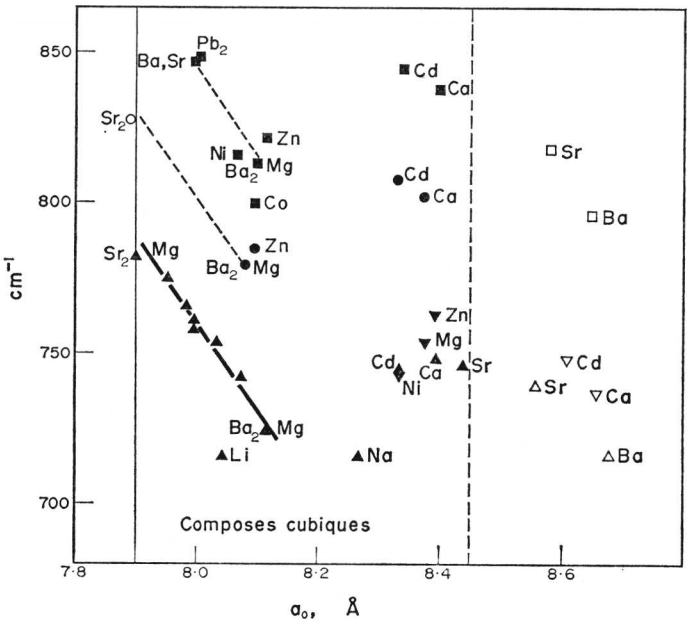

Fig. 4. Relationship between the A_{1g} frequencies (cm^{-1}) and the unit cell parameter a_0 (Å).

Tungstates	■ (cubic)	□ pseudocubic
Molybdates	● (cubic)	○ pseudocubic
Uranates	▼ (cubic)	▽ pseudocubic
Tellurates	▲ (cubic)	△ pseudocubic

(3) The preceding point may be precised by considering the fact that, during the A_{1g} vibration, the oxygen is moving along the B^{VI}—O—B^{II} line (whereas the B cations are at rest).

By combining points (1), (2) and (3), we find that the vibrational frequency is proportional to the B^{VI}—O and B^{II}—O bonding energy and may be expressed, in a simplified way, by a relation of the type:

$$\nu_{A_{1g}} \div \sqrt{E_1 + E_2} \tag{1}$$

where E_1 and E_2 are the B^{VI}—O and B^{II}—O bonding energies.

Taking into consideration the variation of the B^{II}—O distance with the size of the A cation (see above), it may be finally concluded that the frequency variation under discussion is essentially related to the variation of the B^{II}—O distance when the size of the A cation is modified.

Influence of the nature of the hexavalent, octahedral B^{VI} cation

It is evident (Table 7) that, for a given B^{II} cation but different B^{VI} cations, there is no relationship between the A_{1g} frequency and the cell parameter a_0: for similar or equal values of a_0, the A_{1g} frequencies are lower for molybdates than

Table 7. A_{1g} mode frequencies

Compound \ $B^{II}[a_0(Å)]$	Ni	Mg	Zn	Cd	Ca
Ba_2BTeO_6	Hex	724 (8·11)	Hex	745 (8·34)	748 (8·40)
Ba_2BUO_6	743 (8·33)	753 (8·38)	762 (8·39)	d	d
Ba_2BMoO_6	c	779 (8·08)	785 (8·09)	808 (8·33)	802 (8·38)
Ba_2BWO_6	816 (8·07)	813 (8·10)	822 (8·12)	845 (8·34)	838 (8·40)

Hex = hexagonal perovskite
d = distorted phase
c = coloured compound

for tungstates, and still much lower for the corresponding tellurates. Thus, the frequency of the A_{1g} mode is primarily determined by the chemical nature of the hexavalent B^{VI} cation, the bonding energy E_1 in Equation (1) following the sequence W—O > Mo—O > U—O > Te—O. The peculiar behaviour of the Te—O bonds also appears in other physical properties such as the electronic spectra [13] and this may be correlated with the d^{10} electronic configuration of the Te^{VI} cation, in contrast with the d^0 configuration of W^{VI}, Mo^{VI} or U^{VI} cations. Since the d orbitals are fully occupied, a d^{10} configuration is energetically unfavourable to the formation of π bonding between the cation and the oxygen; on the contrary, the d^0 configuration of the other hexavalent cations (W, Mo, U) allows the overlap of the t_{2g} orbitals of the metal and of the ligand orbitals, with as a consequence a strong π-type polarization, and an increase of the B^{VI}—O bonding energy. This explains the large difference between the A_{1g} frequencies of the corresponding tungstates and tellurates.

Influence of the nature of the bivalent, octahedral cation B^{II}

After Equation (1), the A_{1g} frequency is necessarily influenced by the nature of the bivalent B^{II} cation, and this is indeed the case (Fig. 4 and Table 7). But since $E_2 \ll E_1$, this influence is small as compared with that of the hexavalent B^{VI} cation. This problem cannot be handled quantitatively, owing to the lack of information about the B^{II}—O and B^{VI}—O distances and bonding forces. Nevertheless, some specific points may be discussed.

(1) Let us first consider 2 tellurates, namely $(Pb_{1,5}Ba_{05})MgTeO_6$ and $BaLaLiTeO_6$, which have been chosen as having the same value of the cell parameter a_0 (so as to eliminate any spurious effect due to significant differences in the a_0 values). The A_{1g} frequency is 753 cm^{-1} for the former, and 716 cm^{-1} for the latter: this frequency shift probably reflects the lowering of the E_2 bonding energy in Equation (1) when passing from the divalent Mg to the monovalent Li cation, and also shows that the contribution of E_2 to the total restoring force is small, although not negligible, with respect to E_1. If the E_2 bonding energy was negligibly small, the A_{1g} mode could really be described as the totally symmetric stretch of the $B^{VI}O_6$ octahedron, and this description will remain a satisfactory approximation as far as $E_1 \gg E_2$. The actual results show that this condition is fulfilled for the $A_2B^{II}B^{VI}O_6$ compounds investigated here, owing to the large valency difference between the 2 octahedral B cations. But this description of the A_{1g} mode could not be extended

without much care to complex perovskites of the type $Ba_2B^{III}B^{V}O_6$ (such as Ba_2YNbO_6), where the valency difference between the octahedral cations is not large: in this case, the contribution from E_2 to the overall restoring force is far from being small, and the description of the A_{1g} mode as a vibration of the NbO_6 octahedron could only be considered as a very rough approximation.

(2) A useful comparison is also given by the tungstates Ba_2NiWO_6 and Ba_2CoWO_6, since there are among the very few compounds for which the oxygen position has been accurately determined [9]. For these compounds, the cell parameters a_0 are slightly different, but the W–O distances are the same (Table 6), thus eliminating the influence of one of the factors which determine the A_{1g} frequency: thus, the frequency difference (16 cm^{-1}) is really reflecting the specific influence of the bivalent cation. Here again, the frequency difference is small, thus supporting the approximation that the observed frequency is predominantly determined by the WO_6 octahedron.

(3) Finally, it should be remembered that, besides moderately small cations such as Mg, Co, Zn, . . . (whose ionic radius is similar to that of the hexavalent cation), the octahedral sites may also accommodate other bivalent cations such as Cd, Ca, Sr, Ba whose ionic radius is significantly or even considerably larger than the ionic radius of the hexavalent cation. For these compounds, the frequency values of the A_{1g} mode appear to be systematically higher than the values expected from the relationship between the A_{1g} frequency and the cell parameter a_0 (e.g. the A_{1g} frequencies are much higher for the Cd compounds than for their Mg homologs, despite the larger value of the cell parameter—see Table 5). This may be qualitatively explained by the fact that the introduction of too large a bivalent cation on the octahedral site brings out a compression of the adjacent octahedral group, and thus a shortening of the hexavalent cation–oxygen distance, with as a consequence an increase of the vibrational frequency. Such a shortening has been observed for a few Ba compounds (Table 6.).

If, however, this shortening was the only factor to be considered, this would lead to higher and higher A_{1g} frequencies in the series of the Cd, Ca, Sr and Ba compounds, a prediction which is not verified by the experimental results. It appears that large cations such as Sr and Ba can be accommodated in the octahedral holes only by pushing the oxygen outside the B^{VI}—O—B^{II} line. This bending of the B^{VI}—O—B^{II} bond implies a decrease of the overall restoring force and thus of the vibrational frequency.

It may be concluded that, for the perovskites under consideration, the A_{1g} frequency is essentially determined by the nature of the B^{VI} hexavalent cation, this mode being satisfactorily described as the totally symmetric stretch of the $B^{VI}O_6$ octahedron. There is, in addition, a significant influence of the B^{II} bivalent octahedral cation, acting through its own bonding force and ionic radius, and a secondary, but not negligible, influence of the large cation.

E_g mode

Here again, all the cations are necessarily at rest, the oxygen atoms are moving along the B^{VI}—O—B^{II} line (Fig. 5.), and the frequency values should be determined by the B^{VI}—O and B^{II}—O bonding forces and distances. This vibration could

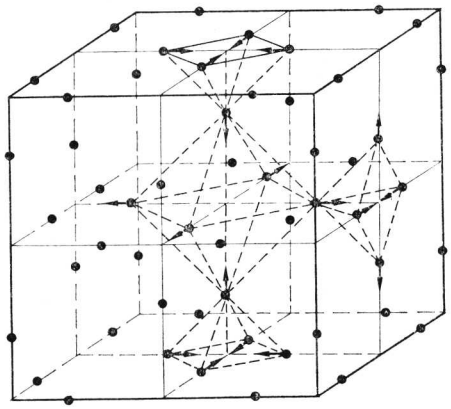

Fig. 5. Symmetry coordinate $S^{E_g} = 1/2\sqrt{3}\ (2z_3 - 2z_6 + y_4 - y_1 + x_2 - x_5)$.

approximately be described as the ν_2 mode of the free $B^{VI}O_6$ octahedral group. Unfortunately, the corresponding band is missing in most spectra, and it is thus impossible to discuss the essential factors which determine its frequency. Nevertheless, one point should be mentioned, namely the splitting of this mode for some tellurate solid solutions (Table 5). The true origin of this splitting is still obscure.

T_{2g} modes

These 2 modes are characterized by the allowed translation of the large A cation (Sr, Pb, Ba). Indeed, such a translation seems to be one of the determining factors for the lowest-lying frequency, in the 150–50 cm^{-1} region. For a series of compounds corresponding to the same A cation (Ba), the frequency values are essentially related to the cell parameter a_0, irrespective of the chemical nature of the B^{VI}

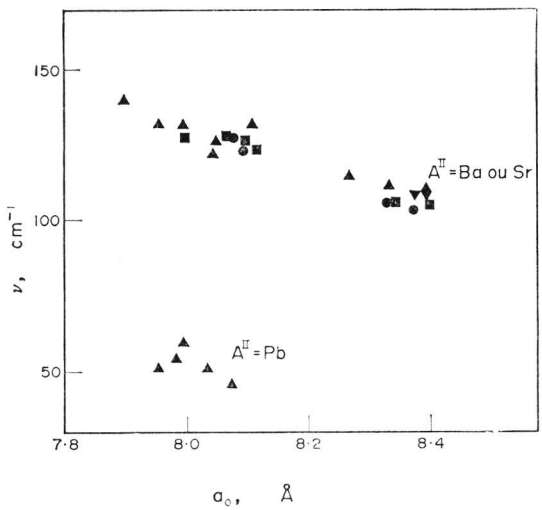

Fig. 6. Relationship between the T_{2g} low frequencies (150–50 cm^{-1}) and the unit cell parameter a_0 (Å).

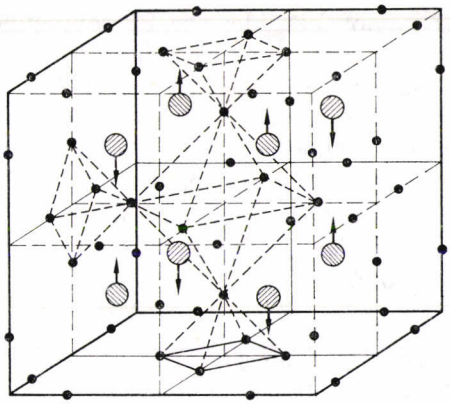

Fig. 7. Normal coordinate $Q^{T_{2g}}$ along z axis $Q_z^{T_{2g}} = v(z_{A_1} - z_{A_2})$.

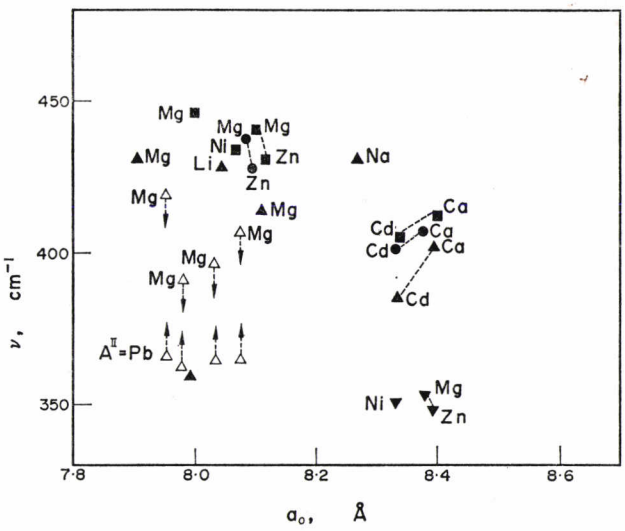

Fig. 8. Relationship between the T_{2g} frequencies (450–350 cm^{-1}) and the unit cell parameter a_0(Å).

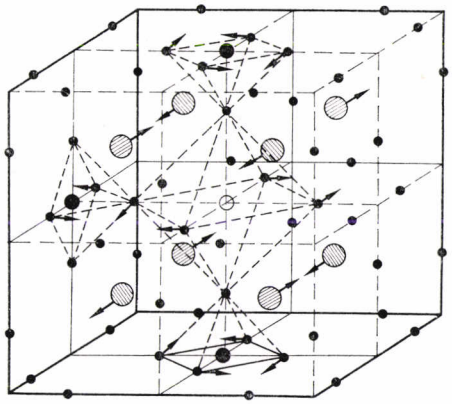

Fig. 9. Normal coordinate $Q^{T_{2g}} = \alpha(x_1 - x_4 + y_5 - y_2) + \beta(x_{A_1} - x_{A_2})$.

and B^{II} cations. But if we now consider the Pb compounds, we find a very large decrease of the frequency which can be explained only by a mass effect of the A cation (Fig. 6). Such a motion is represented in Fig. 7.

This mass effect is considerably reduced for the remaining T_{2g} mode observed in the 450–350 cm^{-1} region. Moreover, for a given A cation, this frequency is not simply related to the cell parameter a_0, but is also influenced by the nature of the B^{VI} and of the B^{II} cations (Fig. 8). As a first (and fairly rough) approximation, this mode may be described as the symmetric bend of the $B^{VI}O_6$ group (ν_5 of a free octahedron), combined with a non-negligible translation of the A cation (Fig. 9).

Acknowledgements—We gratefully acknowledge the financial support given to our laboratory by the Fonds National Belge de la Recherche Scientifique, and the Fonds de la Recherche Fondamentale Collective.